Article

Mineralogical and Microstructural Features of Namibia Marbles: Insights about Tremolite Related to Natural Asbestos Occurrences

Rosalda Punturo [1,*], Claudia Ricchiuti [1], Marzia Rizzo [2] and Elena Marrocchino [2]

[1] Department of Biological, Geological and Environmental Sciences, University of Catania, Corso Italia 55, 95129 Catania, Italy; claudia.ricchiuti@unict.it

[2] Department of Physics and Earth Science—University of Ferrara, Via Saragat 1, 44122 Ferrara, Italy; marzia.rizzo@unife.it (M.R.); mrrlne@unife.it (E.M.)

* Correspondence: punturo@unict.it; Tel.: +39-095-719-5757

Abstract: The Mg-rich marbles of Precambrian rocks of Namibia are widely exploited and marketed abroad for ornamental purposes. Karibib marbles, named after the locality where the most important quarries are located, are commercially known as "White Rhino Marble". They formed under greenschist facies metamorphic conditions and may be characterized by the presence of veins of tremolite. Although the quarries, whose exploited marbles contain tremolite, do not seem to be abundant, we decided to carry out a detailed mineralogical and petrographic study on Karibib marbles in order to point out the occurrence of tremolite, whose shape may vary from prismatic to acicular, even sometimes resembling the asbestiform habitus and its geometry within the rock. With this aim, we carried out optical microscopy, X-ray diffractometry, X-ray scanning electron microscopy, and micro-Raman investigations, and also imaged the 3D fabric with micro computed X-ray tomography. The study of white marbles from Namibia and their mineral phases has an important impact, since tremolite might split into thin fibers and, therefore, being potentially harmful, the presence of tremolite requires an analysis of the risks of exposure to asbestos.

Keywords: rhino white marble of Namibia; tremolite; fibrous habitus; health hazard

1. Introduction

In the last century, Namibia has been one of the favorable mining contexts for the exploration and evaluation of geo-resources. From 1990 to 2000, in Namibia, the production of marble and granite was about 20,000 tons per year. Since 2004, thanks to modern methods and processing machinery, there has been a continuous increase in production, and the production has exceeded the threshold of 50,000 tons/year [1]. The geo-mining industry of Namibia includes several ornamental stones: marbles (calcite and/or dolomite-bearing metacarbonate rocks); magmatic rocks such as granites, granodiorites, and gabbros; serpentinites; and onyxes and alabasters. The firms linked to the ornamental stone that are gathered around the Karibib have become a benchmark for the high quantity and quality of marble.

Since 1900, railway construction has led to great development in mining and, in the past 10 years, the Karibib has become one of the most productive international marble districts that includes extraction, processing, and marketing activities of marble and granite rocks.

In the Karibib district, the most important marble and granite reserves are located in the Karibib quarry area of the northwest sector of town, where the White Rhino and Karibib marble varieties are exploited; in the Nonidas quarry area, which consists of small extractive sites that sit between the northern part of the town of Nonidas and the eastern area of Swakopmund; and the Arandis quarry

area, where the extraction activities mainly concern the domes of intrusive magmatic rocks (pink granite).

At present, there is growing interest due to the ornamental exploitation of these Neoproterozoic carbonate rocks, and many quarries are contributing to the socio-economic development of Namibia and other regions—indeed, extensive outcrops of carbonate rocks are part of Namibia's geological resources and are therefore recalling the interest of mining companies (see also the website of the Namibian Ministry of Mines and Energy [2]).

In this work, mineralogical and petrographic characteristics of the main commercial marble in the Karibib area, known as "Rhino White Marble", are described. It is a dolomite-bearing marble from the Neoproterozoic, which belongs to the Swakop group (Damara sequence). It is exploited and marketed in many European countries, and it is appreciated because of its pearly white appearance, sometimes cut by creamy yellow veins. However, some concerns related to the commercial use of Rhino White Marble are due to the occurrence of tremolite-rich veins, as revealed by preliminary petrographic investigation [3]. Indeed, tremolite, $Ca_2Mg_5Si_8O_{22}(OH)_2$, belongs to the calcic amphibole group of minerals and, when occurring with fibrous habitus, it is considered a dangerous naturally-occurring asbestos—a term applied to six specific silicate minerals that also comprises tremolite—the critical dimension is: length > 5 μm, diameter < 3 μm, length:diameter > 3:1 [4–6].

This mineral usually occurs with elongated and/or bladed prismatic habitus, but it may also be acicular or even fibrous-shaped. According to the literature, tremolite toxicology, as for all asbestos minerals, has been associated with size, durability, and chemical composition (e.g., [7–15]). According to [16], "In mineralogy, acicular is the term applied to straight, free-standing (i.e., individual) and highly elongated crystals; these ones can be bordered and delimited by crystal faces. As far as the acicular crystals, they are characterized by aspect ratio comparable to those ones of fibrous crystals, even though their diameter may extend up to 7 mm". A fiber is defined as an elongate particle that is longer than 5.0 μm, with a minimum aspect ratio (length of the particle divided by its width) of 3:1 [6]. Indeed, when used as building stone, the studied marbles are washed with aggressive detergents and also exposed to accelerated weathering, so the mineral fibers contained within could break and may be spread out in the environment and make them dangerous for the environment and human health [17–26].

Although the quarries of the Karibib area that sit on tremolite-bearing marbles do not seem to be abundant, we considered it necessary to carry out a detailed mineralogical and microstructural investigation in order to characterize the white marbles of Namibia and to detect the eventual occurrence of asbestos tremolite. For the above reasons, the present study has several implications, since the presence of tremolite with asbestiform habitus might be linked to health problems and asbestosis. Therefore, it is a useful tool for initiating an analysis of the risks to occupational and non-occupational activities concerning the use of the tremolite-bearing marble, providing useful suggestions for safe marble exploitation.

2. Materials and Methods

2.1. Geological Setting and Samples

The Namibia marbles belong to the Neoproterozoic carbonate succession, dating 665 ± 34 million years, which constitute the Pan-African Damara Belt. The latter was generated during the orogenic events that produced the Gondwana supercontinent. The sedimentary successions of the Damara Belt, siliciclastic and carbonate in composition, were deposited in an environment of passive continental margin (i.e., Neoproterozoic rift basins) related to the Rodinia break-up on a global scale. In some sectors, the thickness of deposits exceeds 1000 m [27–30]. According to the literature [31–34], the Damara Belt is considered as an asymmetric double-vergent orogen, which separates the Angola-Congo and Kalahari cratons (Figure 1), formed during the Neoproterozoic to early Paleozoic tectonic events related to the closure of the Damara Ocean. In Namibia, the Damara

Orogen (Figure 1) is constituted by three orogenic belts: The intracontinental Damara belt and the coastal belt, the Kaoko belt, and the Gariep belts [35–38].
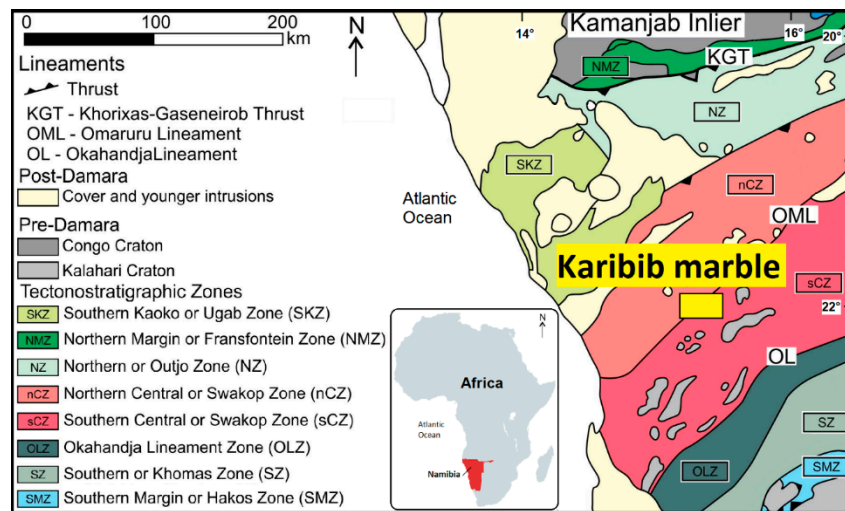

Figure 1. Simplified tectonic map of the Damara Belt (Namibia (Africa). showing the distribution of the main tectono-stratigraphic zones according to [28]. Modified after [35].

In the Central Zone of the Damara Belt, the successions were deformed and metamorphosed to greenschist facies conditions reaching, in some sectors, metamorphic conditions of up to ca. 590 °C and 0.5 GPa [39]. Moreover, a detailed structural mapping [40–45], highlighted as the most striking structural feature of the Central zone, is the northeast trending domes elongated at kilometer-scale [37,40,42,45,46], where the most important quarries are located (Figure 2).
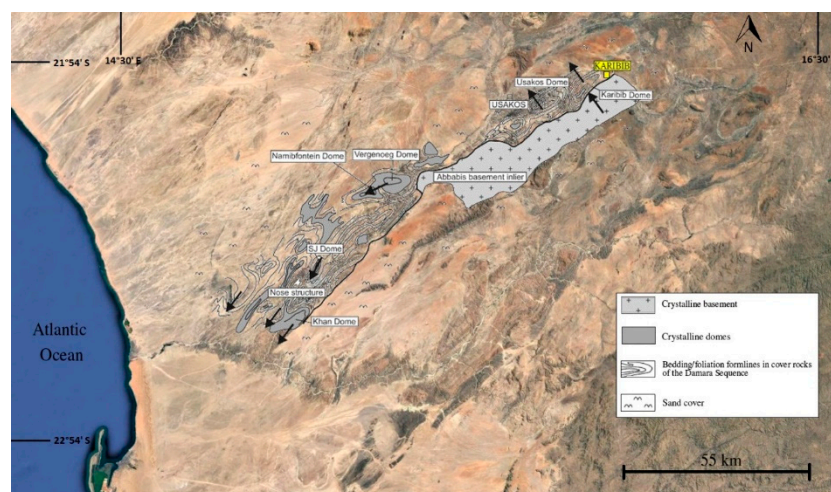

Figure 2. Schematic map showing the northeast trending dome structures covered by the geological map, by [40]. The gneisses and/or the Pan-African granitoids constitute the cores of the dome structures, whereas the surrounding supracrustals of the Damara sequence are draped around the domes. The solid black arrows indicate the tectonic transport direction for domes [41–44] and the Karibib district in the northeast. The yellow rectangle indicates the area where the marble quarries are located.

Deformation and metamorphism have not completely obliterated structures and textures inherited from sedimentary environments, so the planar surfaces due to tectonic deformation overprint the contacts between lithofacies [35,47–49].

Within the carbonate protolith, which represents a pelagic environment with main carbonate sedimentation and a lower contribution of siliceous organisms in relation to the oscillations of Carbonate Compensation Depth, the derived magnesium-rich marbles—which underwent greenschist facies metamorphism—can be characterized by the occurrence of tremolite as one of the main constituting minerals. Conversely, the portions closest to the continental margins do not have tremolite because the Al and Fe terrigenous sediments, metamorphosed under greenschist facies conditions, give chlorite in the metamorphic assemblage.

At the scale of the quarry, White Rhino Marbles of the Karibib area look pearly white and are extracted as dimension stones (Figure 3a)—at the mesoscopic scale, marbles show a saccaroid fabric and are cut by yellowish veins (Figure 3b,c).
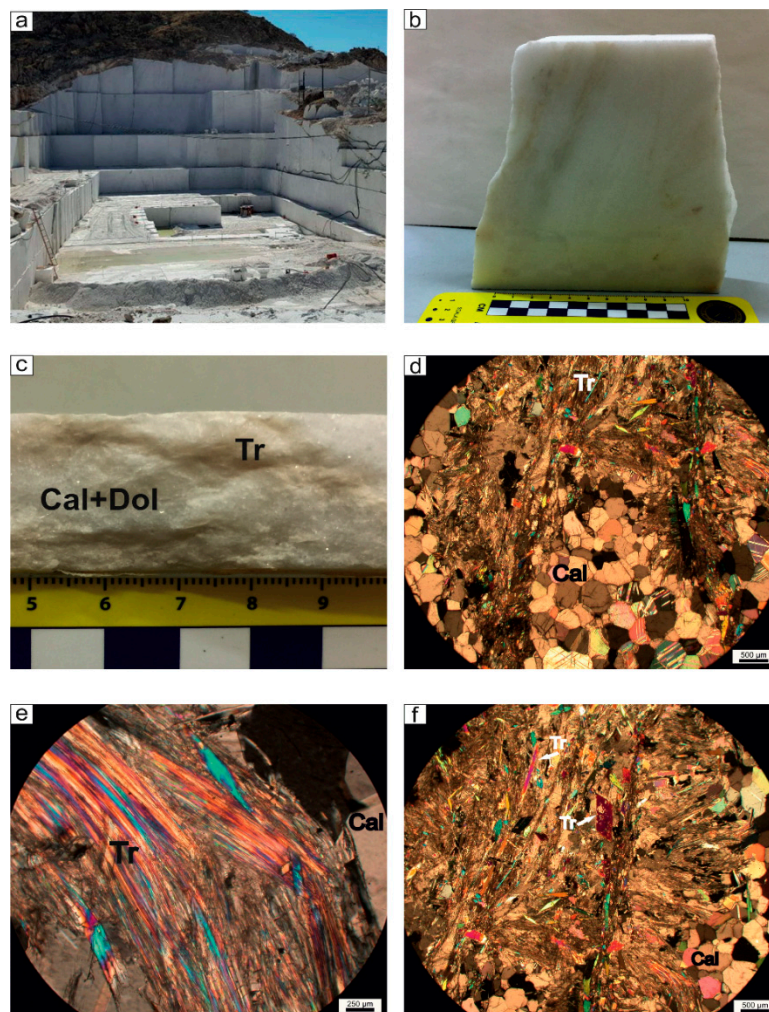

Figure 3. The main features of Karibib white marbles. (**a**) Front of a quarry where marble is exploited as dimensional stone; (**b**) Appearance of the marble at the mesoscopic scale, note the yellow-greenish veins across the pearly portion; (**c**) Particular of a cross section of a brick; (**d**–**f**): Photomicrographs of thin sections of marbles; (**d**) Coexistence of granoblastic portions constituted by calcite with nematoblastic portions constituted by tremolite; (**e**) Blow-up of acicular tremolite-rich level; (**f**) Nematoblastic level showing various habitus types of tremolite, from prismatic to acicular. Mineral symbols after [50].

2.2. Methodologies

In order to describe the microstructural features of the investigated marbles, we selected some specimens for optical microscopy (OM), scanning electron microscopy (SEM/EDS), X-ray diffractometry (XRD), micro-Raman spectrometry, and synchrotron radiation X-ray microtomography

(SR X-ray μCT) investigations. A polarizing microscope Zeiss Axiolab and a Tescan-Vega\\LMU scanning electron microscope (Tescan-Vega, Brno – Kohoutovice, Czech Republic) equipped with an Edax Neptune XM4 60 energy-dispersive X-ray spectrometer (EDS), Edax, Mahwah, NJ, 07430 USA) operating at 20 kV accelerating voltage and 20 nA beam current conditions, were employed to obtain microstructural features, morphoscopic images, and elemental microanalyses. Investigation was carried out on polished thin sections as well as on small chips of marble specimens.

Some specimens were also examined through the X-ray diffractometry (XRD) technique to establish the mineralogical composition. The XRD analysis was performed on rock powder using a Philips PW1860/00 diffractometer (Philips Panalytical Canton, MA, USA), with graphite-filtered Cu Kα radiation (1.54 Å), allowing determination of the mineralogical phases within the constituents. Diffraction patterns were collected in the 2θ angular range 5–50°, with 5 s/step (0.02° 2θ). Moreover, XRD data were quantified by the RIR (Reference Intensity Ratio) method of powder X-ray diffraction data in order to establish the quantities of the constituting minerals according to [51].

A LabRam HR800 micro-Raman instrument from Horiba Jobin Yvon (Horiba, Kyoto, Japan), equipped with an air-cooled CCD detector (1024 × 256 pixels) at −70 °C, an Olympus BXFM microscope, a 600 groove/mm grating, and a 50× objective, was used to collect the Raman scattering signals. The excitation source was a He–Ne laser (632.8 nm line) whose maximum power was 20 mW. The spectrometer was calibrated with silicon at 520 cm^{-1} and the exposure time was varied from 50 to 100 s. Data obtained were compared with the RRUFF^{TM} project database [52]. Moreover, one selected sample considered to be representative of the microstructural features of marbles was imaged by synchrotron radiation X-ray microtomography (SR X-ray μCT) at the SYRMEP (SYnchrotron Radiation for MEdical Physics) beamline of the Elettra synchrotron (Elettra - Sincrotrone Trieste S.C.p.A, Trieste, Italy) in white-beam configuration mode at high spatial resolution. To this aim, we cut a parallelepiped with a size of about 4 mm. The X-ray spectrum was filtered for low energies with 1 mm of Si + 1 mm of Al, and the sample-to-detector distance was set to 200 mm. For each measurement, 1800 projections were acquired over a total scan angle of 180° with an exposure time/projection of 2 s. The detector consisted of a 16-bit air-cooled sCMOS camera (Hamamatsu C11440 22C, Hamamatsu City, Japan) with a 2048°—2048° pixels chip. The effective pixel size of the detector was set at 1.952 μm^2, yielding a maximum field of view of ca. 3.22 mm^2. Since the lateral size of the samples was larger than the detector field of view, the X-ray tomographic microscans were acquired in local or region-of-interest mode [53]. A single distance phase retrieval-preprocessing algorithm [54] was applied to the white beam projections in order to improve the reliability of the quantitative morphological analysis and enhance the image contrast.

The obtained 3D volumes were then imported in VGStudio Max 2.2 (Volume Graphics, Charlotte, NC, USA) for the 3D rendering and segmentation by manual thresholding.

3. Results

At the scale of the microscope, the White Rhino Marbles of the Karibib area had relatively fine grain size with a very heterogeneous distribution of white and yellowish levels, as was revealed by previous mesoscopic observation (Figure 3b,c). Indeed, two main domains, whose thickness ranged from 2 mm up to 1–2 cm, were distinguished on the basis of evident microstructures and constituting minerals: granoblastic levels, given by calcite +/− dolomite (Figure 3d), which are the most abundant portions of the rocks, as also highlighted by mesoscopic observations. Conversely, the nematoblastic levels that occurred to a minor extent, were characterized by tremolite, occurring with various habitus types—indeed, there were levels in which tremolite crystals were made of well-developed prismatic to acicular minerals and minor levels in which this mineral phase tended to constitute fiber belts (Figure 3e,f).

The granoblastic portions, prevalently constituted by calcite and dolomite, showed straight grain boundaries. They were also sutured, even embayed, resulting in an interlocked texture (Figure 3d)—the greenish-yellowish nematoblastic levels, showing marked microstructural anisotropy, were given by

tremolite, occurring as either acicular crystals and/or highly elongated fiber aggregates in belts with radial disposition (Figure 3d,f), together with hetero-granoblastic calcite and dolomite grains elongated parallel to foliation.

XRD and micro-Raman analyses (Figures 4 and 5) showed the coexistence of calcite, tremolite, and dolomite and the absence of other mineral phases also in the finest-grained nematoblastic portions of the yellowish bands, without secondary or accessory minerals occurring. Quantitative phase analyses with the RIR method showed that, on average, the abundances of constituent minerals determined on powders obtained from representative bricks were calcite 70%, tremolite 26%, and dolomite 4%.
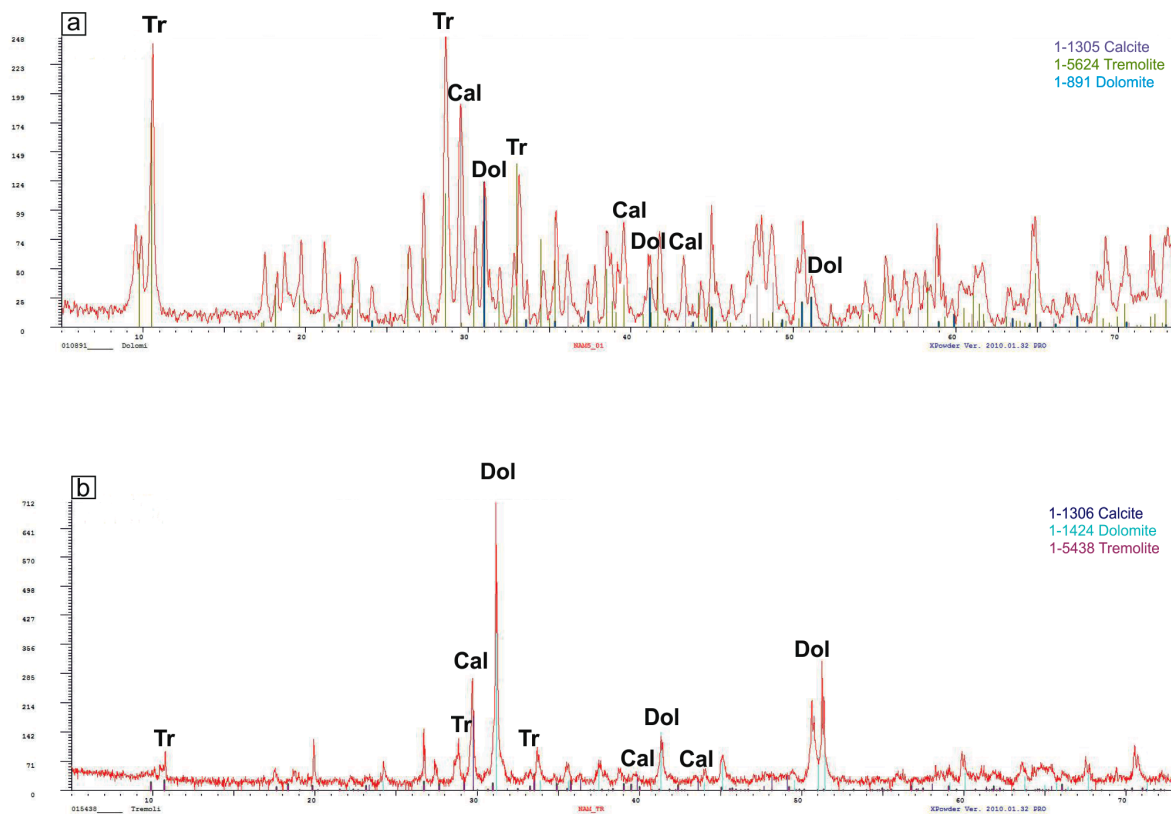

Figure 4. X-ray diffractograms on representative portions of the Karibib white marbles, showing calcite, tremolite, and dolomite as constituting mineral phases. The peak color of each mineral is indicated in the legend. (**a**) main vein; (**b**) massive part.
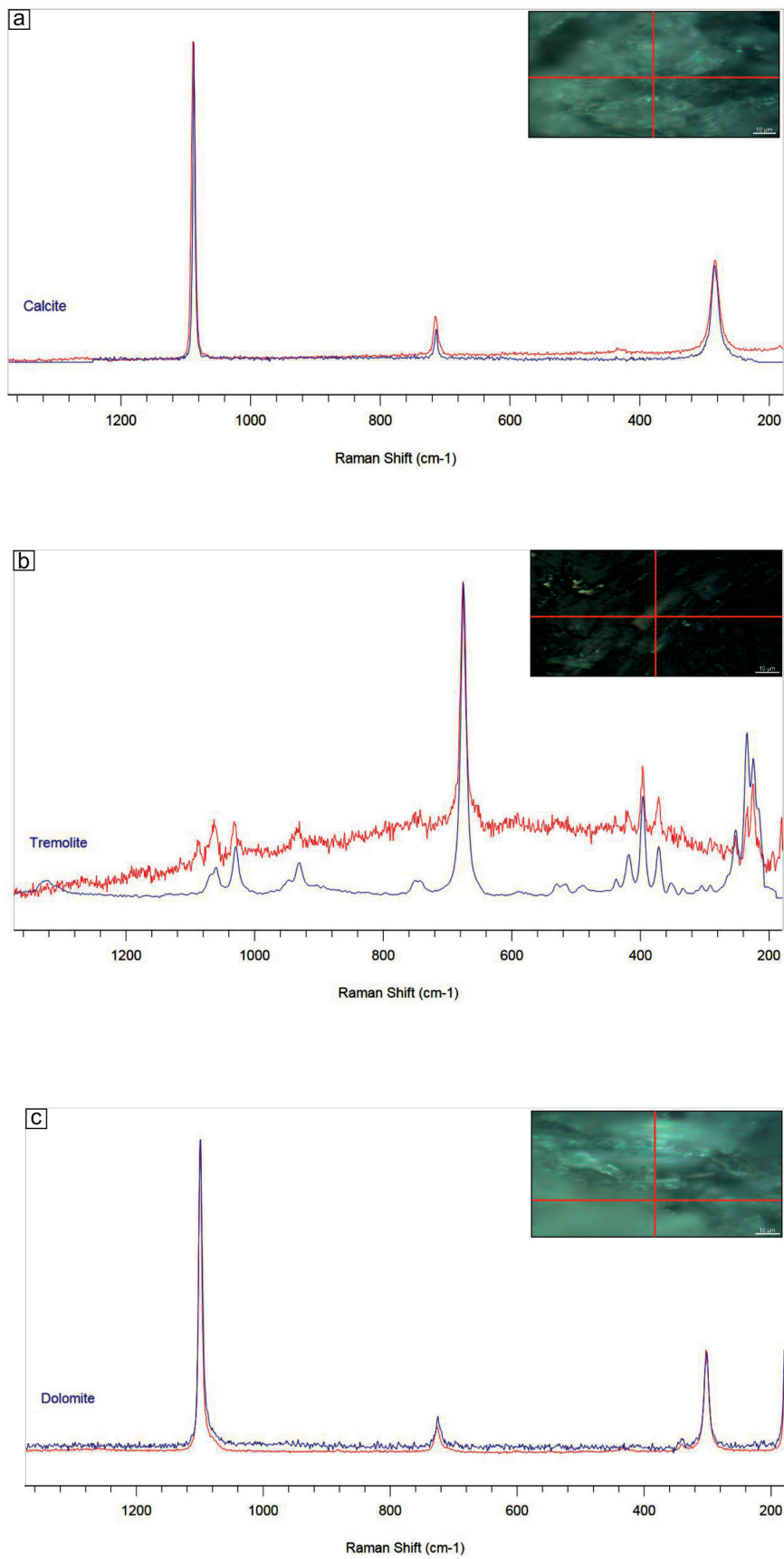
Figure 5. Micro-Raman spectra of selected areas of the Karibib white marbles, showing (**a**) calcite; (**b**) tremolite; and (**c**) dolomite as constituting mineral phases (red spectra). The blue reference spectra are after [52]. Pictures of boxes indicate the investigated points.

The rock exhibited a friable appearance, especially at the contact areas between amphibole and carbonate minerals, with tremolite occurring either with prismatic elongated habitus or elongated fibers, closely bound to carbonate minerals, as can be seen in the SEM images (Figure 6a–c). The SEM/EDS elemental microanalysis suggested that tremolite individuals were pure Mg-member $Ca_2Mg_5(OH)_2Si_8O_{22}$ without any iron detected [55]. Moreover, the SEM images did show that, as a consequence of disaggregation, tremolite might also split into fibers and cleavage fragments, whose shape parameters may resemble asbestiform habitus (Figure 6d–f).
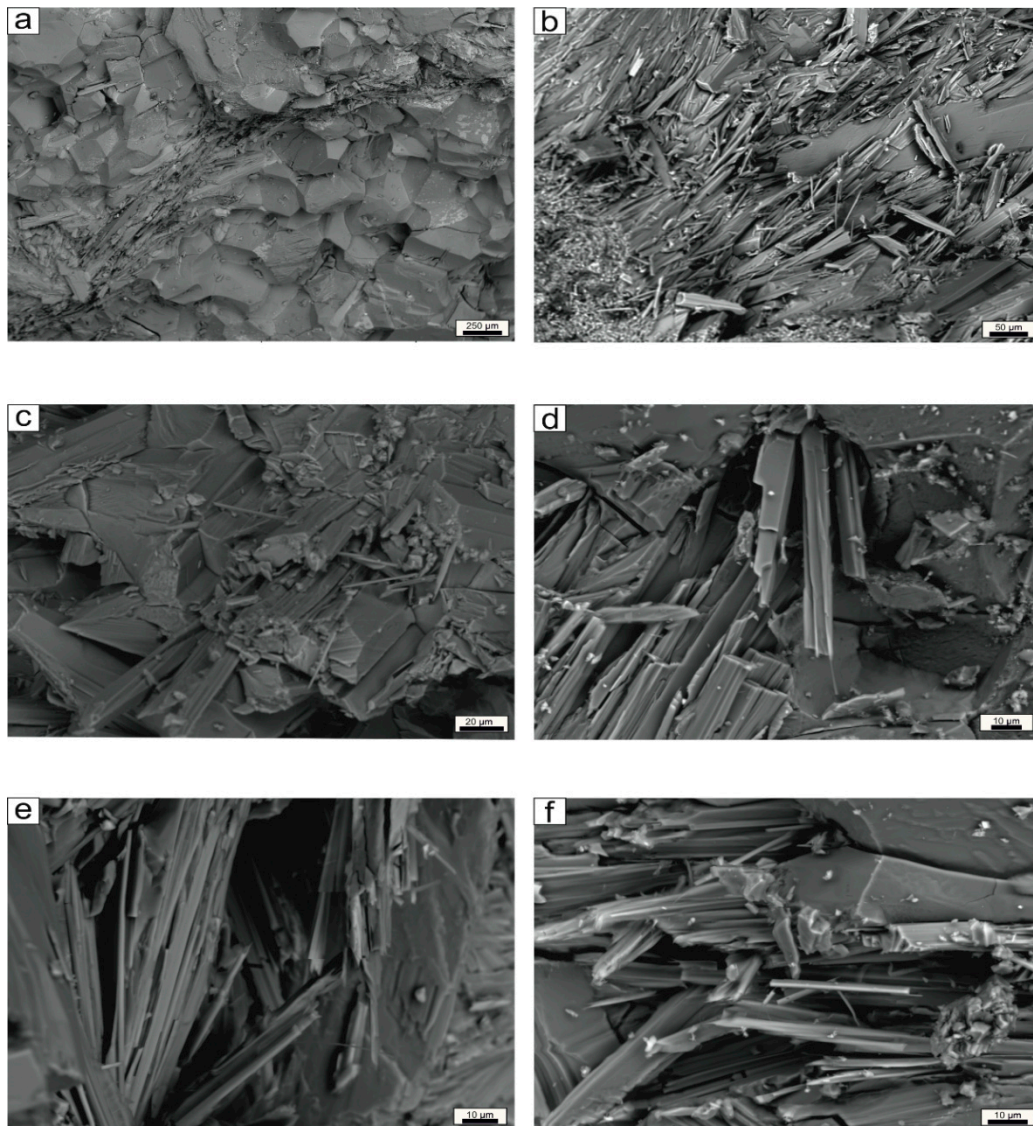

Figure 6. Scanning electron photomicrographs. (**a**) Calcite-rich granoblastic levels cut by tremolite veins; (**b**) Elongated tremolite crystals, sometimes showing radial disposition; (**c**) Tremolite splitting into fibers; (**d**) Tremolite cleavage fragments prone to split; (**e**,**f**) tremolite fibers whose shape parameters may resemble asbestiform habitus. Mineral symbols after [50].

Finally, on one selected small brick measuring about 30 mm × 4 mm, we carried out synchrotron radiation X-ray microtomography (SR X-ray µCT). X-ray microtomography is a non-destructive technique that improves the observation of the arrangement of fibers in the three-dimensional space, thus avoiding any morphological variations of the sample as a result of comminution. Indeed, this technique allowed us to image the three-dimensional enveloping and intergrowth of nematoblastic

and granoblastic levels as well as the geometry and reciprocal arrangement of constituting minerals into the marble, with special regard to the spatial relationship between calcite and tremolite, the latter sometimes showing radial disposition, as can be clearly seen in Figure 7.
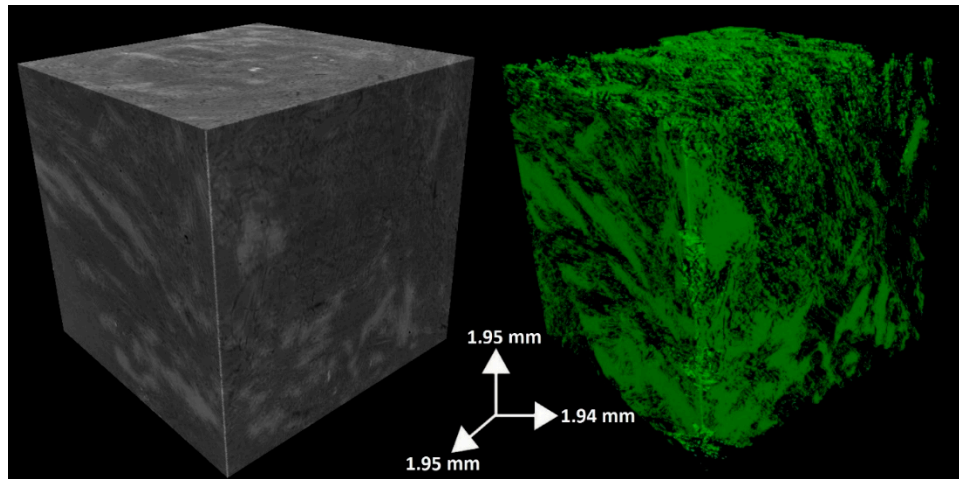

Figure 7. 3D rendering of a selected part of one specimen analyzed by means of synchrotron radiation X-ray micro-tomography: in the left picture, light colors correspond to high-density phases, while dark colors correspond to low-density phases; in the right picture, a green color is associated with the highest-density phase (i.e., tremolite). Note the 3D interlock between tremolite- and carbonate-rich portions.

4. Discussion and Conclusions

The multi-analytical investigation carried out on White Rhino Marbles exploited in the Karibib area (Namibia), which consisted of a detailed petrographic, microstructural, and mineralogical characterization of their fabric and microstructural features, permitted us to highlight the occurrence and to depict the geometry of amphibole minerals in the yellow veins that cut the rock. From the petrological point of view, the Neoproterozoic White Rhino Marbles are characterized by a mineralogical assemblage that proves the absence of terrigenous contributions in their protolith, as they do not contain any aluminum or iron, even in nematoblastic levels in which silicate mineral phases (i.e., amphibole) are found.

During the metamorphic event, the high-silica (e.g., diatomaceous) levels reacted with the Mg-rich carbonates, giving rise to amphibole tremolite $Ca_2Mg_5Si_8O_{22}(OH)_2$. Therefore, the paragenesis of the White Rhino Marbles is given by calcite + tremolite ± dolomite. Calcite and minor dolomite grains are the constituent of the granoblastic levels, which are certainly the most abundant portions of the marble rocks exploited. Conversely, tremolite is the principal constituent of the nematoblastic levels, where it is mainly found with acicular (i.e., needle-like) habitus, which means it is characterized by sectional dimensions that are small relative to its length. Moreover, no secondary minerals formed on primary minerals have been detected or observed, proving that no weathering process has been affecting the studied marbles.

Nevertheless, the detailed microstructural and morphological analyses carried out on marbles highlighted that, despite non-asbestos tremolite exhibiting acicular habitus, it is the most common mineral phase that was found. Asbestos tremolite fibers were also detected within veins. Tremolite-rich veins were easy to distinguish at the mesoscopic and at the optical microscopic scale, where they defined the microstructural anisotropy of marbles. Scanning the electron microscopy highlighted that tremolite fibers, resembling the asbestiform habitus, occurred as fibrous aggregates with radial arrangement, prone to split into thinner fibers and ultimately into fibrils, often formed after cleavage fragments. Despite its occurring habitus, tremolite appeared as straight and stiff crystals (i.e., needles

and fibers). Moreover, 3D imaging showed the tight interlock between the nematoblastic microdomains (i.e., tremolite-rich) and the granoblastic portions (i.e., carbonate-rich) and their contact geometry.

The asbestos hazard related to the occurrence of fibrous tremolite veins that cross-cut the studied marbles arises when either natural weathering processes (e.g., erosion and mobilization) or human activities (e.g., exploitation of dimension blocks and subsequent use as building stones) separate tremolite fibers and break them down, making them dispersed into the environment as airborne and easily breathable.

For instance, during the steps of marble quarrying, non-asbestos tremolite can break along preferred cleavage planes and be released in the air. For this reason, it is ultimately possible for workers to be exposed to asbestos during these activities. Therefore, before any exploitation and subsequent process of marble containing non-asbestos minerals, which may otherwise develop into minerals with asbestiform habitus, it is necessary that mining companies adopt monitoring surveys, in situ tests, as well as safety measures and prevention practices for each recognized hazardous situation. Among them it is worth noting the avoidance of asbestos veins during exploitation, maintenance of devices, use of protective personal equipment, planning sanitary surveillance, and envisaging dust abatement and remediation systems [21,56–58]. As far as the non-occupational point of view states, it is important to assess the extent of exposure to those airborne particles, whose morphology may resemble asbestos, to populations who live close to the quarry as well as to family members of workers. Finally, we suggest that weathering and ageing tests should be carried out on vein-rich marble, in order to detect any deterioration forms that may cause the release of fibers, and to plan eventual remediation practices.

Author Contributions: Each author made substantial individual contribution to the work as follows: Conceptualization, R.P.; methodology and analysis, R.P., C.R., and M.R.; writing, R.P., C.R., M.R., and E.M.; validation, R.P. and E.M.; editing C.R. and E.M.; funding acquisition R.P.

Conflicts of Interest: The authors declare no conflict of interest.

References

1. Ministry of Mines and Energy. Available online: http://www.mme.gov.na (accessed on 20 January 2019).
2. Ministry of Mines and Energy. Available online: http://www.mme.gov.na/directorates/mine/ (accessed on 20 January 2019).
3. Vaccaro, C.; Punturo, R.; Volpe, L.; Marrocchino, E.; Rizzo, M.; Ricchiuti, C.; Mannino, M. *Tremolite—Bearing Marbles from Namibia Exploited as Dimension Stone: Preliminary Mineralogical and Petrographic Characterization*; Abstract Book; Congresso SGI-SIMP: Catania, Italy, 2018.
4. World Health Organization (WHO). *Asbestos and Other Natural Mineral Fibres*; Environmental Health Criteria, 53; World Health Organization: Geneva, Switzerland, 1986; p. 194.
5. National Institute for Occupational Safety and Health (NIOSH). *Asbestos and Other Elongated Mineral Particles: State of the Science and Roadmap for Research*; Revised Draft; NIOSH Current Intelligence Bulletin: Washington, DC, USA, 2008.
6. International Agency for Research on Cancer (IARC). *Asbestos (Chrysotile, Amosite, Crocidolite, Tremolite, Actinolite, and Anthophyllite) IARC Monographs*; Arsenic, Metals, Fibres and Dusts; International Agency for Research on Cancer: Lyon, France, 2009; pp. 147–167.
7. Mossman, B.T.; Lippmann, M.; Hesterberg, T.W.; Kelsey, K.T.; Barchowsky, A.; Bonner, J.C. Pulmonary endpoints (lung carcinomas and asbestosis) following inhalation exposure to asbestos. *J. Toxicol. Environ. Health* **2011**, *14*, 76–121. [CrossRef] [PubMed]

8. Pugnaloni, A.; Giantomassi, F.; Lucarini, G.; Capella, S.; Bloise, A.; Di Primio, R.; Belluso, E. Cytotoxicity induced by exposure to natural and synthetic tremolite asbestos: An in vitro pilot study. *Acta Histochem.* **2013**, *115*, 100–112. [CrossRef] [PubMed]

9. Oberti, R.; Hawthorne, F.C.; Cannillo, E.; Camara, F. Long-range order in amphiboles. In *Amphiboles: Crystal Chemistry, Occurrence, and Health Issues Hawthorne*; Oberti, F.C., della Ventura, R., Mottana, G.A., Eds.; Mineralogical Society of America: Chantilly, VA, USA, 2007; pp. 125–172.

10. Ballirano, P.; Bloise, A.; Gualtieri, A.F.; Lezzerini, M.; Pacella, A.; Perchiazzi, N.; Dogan, M.; Dogan, A.U. The Crystal Structure of Mineral Fibres. In *Mineral Fibres: Crystal Chemistry, Chemical-Physical Properties, Biological Interaction and Toxicity*; Gualtieri, A.F., Ed.; European Mineralogical Union: London, UK, 2017; Volume 18, pp. 17–53.

11. Gaggero, L.; Sanguineti, E.; Yus González, A.; Militello, G.M.; Scuderi, A.; Parisi, G. Airborne asbestos fibres monitoring in tunnel excavation. *J. Environ. Manag.* **2017**, *196*, 583–593. [CrossRef] [PubMed]

12. Apollaro, C.; Fuoco, I.; Vespasiano, G.; De Rosa, R.; Cofone, F.; Miriello, D.; Bloise, A. Geochemical and mineralogical characterization of tremolite asbestos contained in the Gimigliano-Mount Reventino Unit (Calabria, south Italy). *JMES* **2018**, *10*, 5–15. [CrossRef]

13. Punturo, R.; Bloise, A.; Critelli, T.; Catalano, M.; Fazio, E.; Apollaro, C. Environmental implications related to natural asbestos occurrences in the ophiolites of the Gimigliano-Mount Reventino Unit (Calabria, southern Italy). *Int. J. Environ. Res.* **2015**, *9*, 405–418.

14. Constantopoulos, S.H. Environmental mesothelioma associated with tremolite asbestos: Lessons from the experiences of Turkey, Greece, Corsica, New Caledonia and Cyprus. *Regul. Toxicol. Pharmacol.* **2008**, *52*, 110–115. [CrossRef] [PubMed]

15. Bloise, A.; Barca, D.; Gualtieri, A.F.; Pollastri, S.; Belluso, E. Trace elements in hazardous mineral fibres. *Environ. Pollut.* **2016**, *216*, 314–323. [CrossRef]

16. Strohmeier, B.R.; Huntington, J.C.; Bunker, K.L.; Sanchez, M.S.; Allison, K.; Lee, R.J. What is asbestos and why is it important? Challenges of defining and characterizing asbestos. *Int. Geol. Rev.* **2010**, *52*, 801–872. [CrossRef]

17. Petriglieri, J.R.; Laporte-Magoni, C.; Gunkel-Grillon, P.; Tribaudino, M.; Bersani, D.; Sala, O.; Salvioli-Mariani, E. Mineral fibres and environmental monitoring: A comparison of different analytical strategies in new caledonia. *Geosci. Front.* **2019**. [CrossRef]

18. Laporte-Magoni, C.; Petriglieri, J.R.; Gunkel-Grillon, P.; Salvioli-Mariani, E.; Selmaoui-Folcher, N.; Le Mestre, M. Weathering Influence on fiber release of asbestos type minerals under subtropical climate. In Proceedings of the XXII Meeting of the International Mineralogical Association, Melbourne, Australia, 13–17 August 2018.

19. Bloise, A.; Kusiorowski, R.; Lassinantti Gualtieri, M.; Gualtieri, A.F. Thermal behaviour of mineral fibres. In *Mineral Fibres: Crystal Chemistry, Chemical-Physical Properties, Biological Interaction and Toxicity*; Gualtier, A.F., Ed.; European Mineralogical Union: London, UK, 2017; Volume 18, pp. 215–252.

20. Bloise, A.; Punturo, R.; Catalano, M.; Miriello, D.; Cirrincione, R. Naturally occurring asbestos (NOA) in rock and soil and relation with human activities: The monitoring example of selected sites in Calabria (southern Italy). *Ital. J. Geosci.* **2016**, *135*, 268–279. [CrossRef]

21. Bellomo, D.; Gargano, C.; Guercio, A.; Punturo, R.; Rimoldi, B. Workers' risks in asbestos contaminated natural sites. *JMES* **2018**, *10*, 97–106.

22. Pacella, A.; Andreozzi, G.B.; Ballirano, P.; Gianfagna, A. Crystal chemical and structural characterization of fibrous tremolite from Ala di Stura (Lanzo Valley, Italy). *Period. Mineral.* **2008**, *77*, 51–62.

23. Belardi, G.; Vignaroli, G.; Trapasso, F.; Pacella, A.; Passeri, D. Detecting asbestos fibres and cleavage fragments produced after mechanical tests on ophiolite rocks: Clues for the asbestos hazard evaluation. *JMES* **2018**, *10*, 63–78. [CrossRef]

24. Punturo, R.; Cirrincione, R.; Pappalardo, G.; Mineo, S.; Fazio, E.; Bloise, A. Preliminary laboratory characterization of serpentinite rocks from Calabria (southern Italy) employed as stone material. *J. Mediterr. Earth Sci.* **2018**, *10*, 79–87. [CrossRef]

25. Punturo, R.; Ricchiuti, C.; Mengel, K.; Apollaro, C.; De Rosa, R.; Bloise, A. Serpentinite-derived soils in southern Italy: Potential for hazardous exposure. *J. Mediterr. Earth Sci.* **2018**, *10*, 51–61. [CrossRef]

26.　Censi, P.; Zuddas, P.; Randazzo, L.A.; Tamburo, E.; Speziale, S.; Cuttitta, A.; Punturo, R.; Santagata, R. Source and nature of inhaled atmospheric dust from trace element analyses of human bronchial fluids. *Environ. Sci. Technol.* **2011**, *45*, 6262–6267. [CrossRef]

27.　South African Committee for Stratigraphy, SACS. Stratigraphy of South Africa, Part I. Lithostratigraphy of the Republic of South Africa, South West Africa/Namibia and the Republics of Bophuthatswana, Transkei and Venda. *Geol. Surv. S. Afr.* **1980**, *8*, 690.

28.　Kröner, A. Late Precambrian diamictites of South Africa and Namibia. In *Earth's Pre-Pleistocene Glacial Record*; Hambrey, M.J., Harland, W.B., Eds.; Cambridge University Press: Cambridge, UK, 1981; pp. 167–177.

29.　Paciullo, F.V.P.; Ribeiro, A.; Trouw, R.A.J.; Passchier, C.W. Facies and facies association of the siliciclastic Brak River and carbonate Gemsbok formations in the Lower Ugab River valley, Namibia, W. *Africa. J. Afr. Earth Sci.* **2007**, *47*, 121–134. [CrossRef]

30.　Miller, R.M. Neoproterozoic and early Palaeozoic rocks of the Damara Orogen. In *The Geology of Namibia*, 2nd ed.; Miller, R.M., Ed.; Geological Survey of Namibia: Windhoek, Namibia, 2008; pp. 1311–1341.

31.　Hoffmann, K.H. *Sedimentary Depositional History of the Damara Belt Related to Continental Breakup, Passive to Active Margin Transition and Foreland Basin Development*; Abstract of the 23rd Earth Science Congress; Geological Society of South Africa: Cape Town, South Africa, 1990; pp. 250–253.

32.　Kukla, P.A.; Stanistreet, I.G. Record of the Damara Khomas Hochland accretionary prism in central Namibia: Refutation of an "ensialic" origin of a Late Proterozoic orogenic belt. *Geology* **1991**, *19*, 473–476. [CrossRef]

33.　Kukla, P.A. Tectonics and sedimentation of a late Proterozoic Damaran convergent continental margin, Khomas Hochland. *Memoir. Geol. Surv. Namib.* **1992**, *12*, 1–95.

34.　Blanco, G.; Germs, G.J.B.; Rajesh, H.M.; Chemale, F., Jr.; Dussin, I.A.; Justino, D. Provenance and paleogeography of the Nama Group (Ediacaran to early Paleozoic, Namibia): Petrography, geochemistry and U-Pb detrital zircon geochronology. *Precambr. Res.* **2011**, *187*, 15–32. [CrossRef]

35.　Nascimento, D.B.; Ribeiro, A.; Trouw, R.A.J.; Schmitt, R.S.; Passchier, C.W. Stratigraphy of the Neoproterozoic Damara Sequence in northwest Namibia: Slope to basin sub-marine mass-transport deposits and olistolith fields. *Precambr. Res* **2016**, *278*, 108–125. [CrossRef]

36.　Porada, H. The Damara-Ribeira orogen of the Pan-African/Brasiliano cycle in Namibia (South West Africa) and Brazil as interpreted in terms of continental collision. *Tectonophysics* **1979**, *57*, 237–265. [CrossRef]

37.　Miller, R.M. The Pan-African Damara orogen of south west Africa/Namibia. In *Evolution of the Damara Orogen of South West Africa/Namibia*; Miller, R.M., Ed.; The Geological Society of South Africa: Johannesburg, South Africa, 1983; Volume 11, pp. 431–515.

38.　Prave, A.R. Tale of three cratons: Tectostratigraphic anatomy of the Damara Orogen in northwestern Namibia and the assembly of Gondwana. *Geology* **1996**, *24*, 1115–1118. [CrossRef]

39.　Puhan, D. Reverse age relations of talc and tremolite deduced from reaction textures in metamorphosed siliceous dolomites of the southern Damara Orogen (Namibia). *Contrib. Mineral. Petrol.* **1988**, *98*, 24–27. [CrossRef]

40.　Smith, D.A.M. The geology around the Khan and Swakop Rivers in South West Africa. *Memoir. Geol. Surv. S. Afr. S.W. Afr. Ser.* **1965**, *3*, 113.

41.　Jacob, R.E.; Snowden, P.A.; Bunting, F.J.L. Geology and structural development of the tumas basement dome and its cover rocks. In *Evolution of the Damara Orogen of South West Africa/Namibia*; Milled, R.M., Ed.; Geological Society of South Africa, Special Publisher: Johannesburg, South Africa, 1983; Volume 11, pp. 157–172.

42.　Kröner, A. Dome structures and basement reactivation in the Pan-African Damara belt of Namibia/South West Africa. In *Precambrian Tectonics Illustrated*; Kröner, A., Greiling, R.O., Eds.; Naegele and Obermiller: Stuttgart, Germany, 1984; pp. 191–206.

43.　Oliver, G.J.H. Mid-crustal detachment and domes in the central zone of the Damara Orogen, Namibia. *J. Afr. Earth Sci.* **1994**, *19*, 331–344. [CrossRef]

44.　Poli, L.C.; Oliver, G.J.H. Constrictional deformation in the Central Zone of the Damara Orogen, Namibia. *J. Afr. Earth Sci.* **2001**, *33*, 303–321. [CrossRef]

45.　Alexander, F.M.; Kisters, L.; Smith, J.; Kathrin, N. Thrust-related dome structures in the Karibib district and the origin of orthogonal fabric domains in the south Central Zone of the Pan-African Damara belt, Namibia. *Precambri. Res* **2004**, *133*, 283–303. [CrossRef]

46.　Jacob, R.E. Geology and Metamorphic Petrology of Part of the Damara Orogen along the Lower Swarkop River, South West Africa. Bulletin of the Precambrian res Unit. Ph.D. Thesis, University of Cape Town, Cape Town, South Africa, 1974.

47.　Smith, E.F.; MacDonald, F.A.; Crowley, J.L.; Hodgin, E.B.; Schrag, D.P. Tectonostratigraphic evolution of the *c*. 780–730 Ma Beck Spring Dolomite: Basin Formation in the core of Rodinia. *Geol. Soc. Lond.* **2016**, *424*, 213–239. [CrossRef]

48.　Marian, M.L. Sedimentology of the Beck Spring Dolomite, Eastern Mojave Desert, California. Master's Thesis, University of Southern California, Los Angeles, CA, USA, 1979.

49.　Corsetti, F.A.; Kaufman, A.J. Stratigraphic investigations of carbon isotope anomalies and Neoproterozoic ice ages in Death Valley, California. *Geol. Soc. Am. Bull.* **2003**, *115*, 916–932. [CrossRef]

50.　Whitney, D.L.; Evans, B.W. Abbreviations for names of rock-forming minerals. *Am. Mineral.* **2010**, *95*, 185–187. [CrossRef]

51.　Hubbard, C.R.; Snyder, R.L. RIR-measurement and use in quantitative XRD. *Powder Diffr.* **1988**, *3*, 74–77.

52.　RRUFF™ Project Database. Available online: http://rruff.info/ (accessed on 20 February 2019).

53.　Maire, E.; Withers, P.J. Quantitative X-ray tomography. *Int. Mater. Rev.* **2014**, *59*, 1–43. [CrossRef]

54.　Paganin, D.; Mayo, S.C.; Gureyev, T.E.; Miller, P.R.; Wilkins, S.W. Simultaneous phase and amplitude extraction from a single defocused image of a homogeneous object. *J. Microsc.* **2002**. [CrossRef]

55.　Leake, B.E.; Woolley, A.R.; Arps, C.E.; Birch, W.D.; Gilbert, M.C.; Grice, J.D.; Hawthorne, F.C.; Kato, A.; Kisch, H.J.; Krivovichev, V.G.; et al. Nomenclature of amphiboles: Report of the subcommittee on amphiboles of the international mineralogical association, commission on new minerals and mineral names. *Can. Mineral.* **1997**, *35*, 219–246.

56.　Witek, J.; Psiuk, B.; Naziemiec, Z.; Kusiorowski, R. Obtaining an artificial aggregate from cement-asbestos waste by the melting technique in an arc-resistance furnace. *Fibers* **2019**, *7*, 10. [CrossRef]

57.　Witek, J.; Kusiorowski, R. Neutralization of cement-asbestos waste by melting in an arc-resistance furnace. *Waste Manag.* **2017**, *69*, 336–345. [CrossRef]

58.　Spasiano, D.; Pirozzi, F. Treatments of asbestos containing wastes. *J. Environ. Manag.* **2017**, *204*, 82–91. [CrossRef]